Chemical Science

ROYAL SOCIETY OF CHEMISTRY

EDGE ARTICLE

View Article Online
View Journal | View Issue

Cite this: *Chem. Sci.*, 2025, **16**, 13838

All publication charges for this article have been paid for by the Royal Society of Chemistry

Received 29th March 2025
Accepted 22nd June 2025

DOI: 10.1039/d5sc02378e

rsc.li/chemical-science

Thermal proteome profiling of itaconate interactome in macrophages†

Yunzhu Meng,‡[ab] Tiantian Wei,‡[acd] Chenlin Zhang,[ab] Anqi Yu,[ab] Yuan Liu,[ab] Junyu Xiao[ad] and Chu Wang *[abe]

Itaconate (ITA) is an upregulated immunometabolite in macrophages during pathogen infection. It is known to influence oxidation stress, cellular metabolism, programmed cell death and many other biological processes to regulate the immune response *via* interaction with proteins. Previous studies capture covalently ITA-modified proteins by activity-based proteome profiling with bioorthogonal chemical probes; however, how itaconate interacts non-covalently with other proteins at the proteome level remains unexplored. Here we applied thermal proteome profiling (TPP) to globally identify a large number of ITA-interacting proteins in macrophage proteomes. Among these targets, we verified mitochondrial branched-chain aminotransferase (BCAT2) as a novel non-covalent binding target of itaconate *via* biochemical and structural experiments. The binding of itaconate could inhibit transamination activity of BCAT and regulate the metabolism of branched-chain amino acids (BCAAs) in lipopolysaccharide (LPS)-activated inflammatory macrophages. This study offers a valuable resource that helps decipher novel and comprehensive functions of ITA in macrophages during the immune response and other related biological processes.

Introduction

Macrophages are one of the key immune cell types that defend against pathogen invasion. Upon pathogenic signal stimulation, they undergo a series of changes such as upregulating the transcription of particular genes and reprogramming metabolic processes.[1,2] Itaconate (ITA) is a by-product of the tricarboxylic acid (TCA) cycle catalyzed by aconitate decarboxylase 1 (ACOD1),[3] which is significantly up-regulated and plays a crucial regulatory role during pathogen infection (Fig. 1a).[2,4,5] This immunoregulatory metabolite has been reported to help hosts defend against pathogen infection,[6–8] and affect cell metabolism,[9,10] redox homeostasis,[11] and signal transduction.[12,13] Recent studies have also highlighted the versatile roles of itaconate in moderating effects on epigenetics[14] and obesity.[15–17]

Itaconate accomplishes these regulatory roles by interacting with important proteins primarily through covalent modification.[5] As itaconate has an electrophilic double bond, it can modify the cysteine residues in proteins *via* Michael addition, which is a process known as "itaconation".[18] Since the discovery of itaconation on KEAP1 in 2018,[13] a series of chemical probes and proteomic methods have been developed to identify itaconation proteins and sites in macrophages[18,19] and pathogens,[20,21] which have greatly promoted functional investigation of itaconate.[12,22] More recently, an ITA-mediated lysine acylation was discovered whose functional impact is yet to be investigated.[23]

In addition to covalent modification, itaconate has also been shown to non-covalently interact with certain proteins and affect their functions. For example, succinate dehydrogenase (SDH)[9] and Tet methylcytosine dioxygenase 2 (TET2)[14] are two non-covalent interacting proteins of itaconate. In both cases, itaconate binds to the proteins' substrate-binding pockets mainly through dicarboxylic groups, mimicking the action of their native substrates of succinate[24] and α-ketoglutarate (AKG),[14] respectively. These non-covalent interactions between itaconate and the target proteins resulted in the suppression of protein activity and regulation of downstream metabolic[9] or transcriptional pathways.[14] However, since the current chemical probes and proteomic methods can only profile the covalent

[a]*Peking-Tsinghua Center for Life Sciences, Academy for Advanced Interdisciplinary Studies, Peking University, Beijing 100871, China. E-mail: chuwang@pku.edu.cn*
[b]*Synthetic and Functional Biomolecules Center, Beijing National Laboratory for Molecular Sciences, Key Laboratory of Bioorganic Chemistry and Molecular Engineering of Ministry of Education, College of Chemistry and Molecular Engineering, Peking University, Beijing 100871, China*
[c]*State Key Laboratory of Natural and Biomimetic Drugs, School of Pharmaceutical Sciences, Peking University, Beijing 100191, China*
[d]*The State Key Laboratory of Protein and Plant Gene Research, School of Life Sciences, Peking University, Beijing 100871, China*
[e]*Peking University Chengdu Academy for Advanced Interdisciplinary Biotechnologies, Chengdu 610231, China*

† Electronic supplementary information (ESI) available: Experimental details and supplemental figures and tables. See DOI: https://doi.org/10.1039/d5sc02378e

‡ These authors contributed equally to this work.

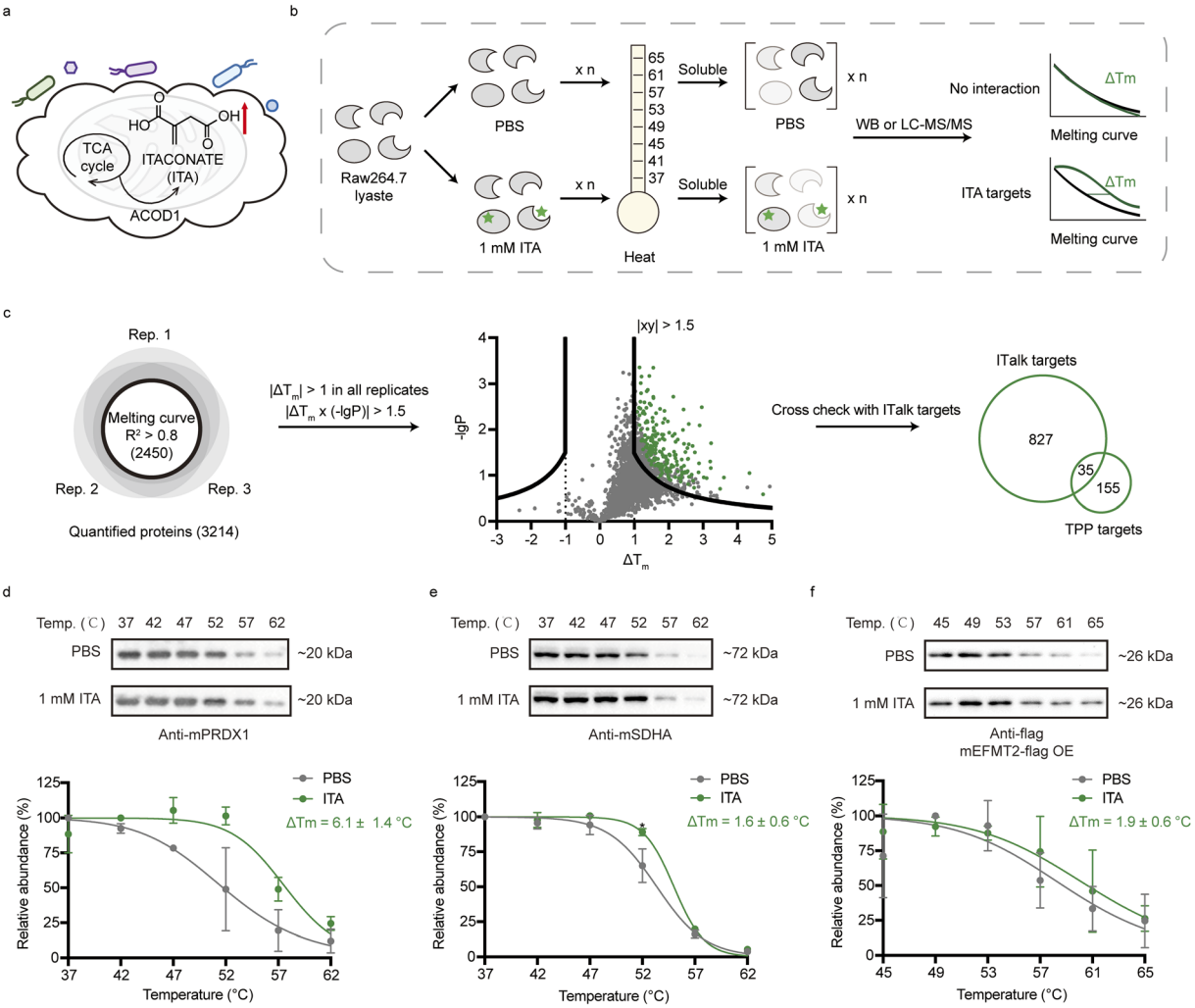

Fig. 1 Profiling of itaconate-interacting proteins by TPP. (a) Itaconate is a key metabolite in macrophages catalyzed by ACOD1 in mitochondria. (b) Scheme of temperature-based TPP for profiling ITA targets. (c) Analysis of TPP data. Left, Venn diagram showing the number of proteins that were quantified in all three biological replicates with good melting curves. Middle, volcano plot showing the proteins with quantified ΔT_m and the associated statistical significance by TPP. Green points represent ITA targets with larger ΔT_m and stronger significance. Right, Venn diagram illustrating the overlap between ITA targets identified by TPP and those captured by ITalk probes through covalent itaconation. (d and e) Thermal stability changes of mouse PRDX1 (d) and SDHA (e) after ITA incubation in RAW 264.7 cell lysate. (f) Thermal stability changes of the overexpressed mouse EFMT2 after ITA incubation in HEK293T cell lysate. In (d–f), immunoblotting and quantification curves are shown at the top and bottom, respectively. Error bars stand for mean ± std, $n = 3$.

targets of itaconate, the non-covalent interactome landscape of itaconate in macrophages is yet to be explored.

Thermal proteome profiling (TPP) is a powerful technology that enables interactome profiling of metabolites or ligands in their native forms.[25–29] Operating based on the rationale that ligand binding or modification to a protein may alter its thermal stability, TPP, as enabled by the multiplex quantitative proteomics (such as TMT), can be used to draw and compare melting curves for thousands of proteins in proteomes simultaneously in the absence *vs.* presence of ligand cotreatment, which can be analysed to identify targets of a ligand molecule at the proteome level.[27] The power of this chemoproteomic technology has been highlighted in numerous applications such as detecting targets of drugs,[25,28,30,31] endogenous metabolites[32–35] and even metal cofactors[36] without derivatization. In addition, it also helps profile targets of post-translational modification such as phosphorylation,[37–39] *O*-GlcNAcylation,[40] and methylation.[41]

Considering that itaconate can both covalently modify and non-covalently interact with proteins, we reasoned that TPP can aid in identification of more ITA-interacting proteins in proteomes, especially those non-covalent binding targets that were previously neglected by probe-based chemoproteomic methods. We therefore applied TPP to globally map itaconate's interactome in macrophage cells. By comparing with the published data for covalently itaconated proteins, we obtained a list of non-covalent targets of itaconate, among which the mitochondrial branched-chain amino acid aminotransferase 2 (BCAT2) was structurally and functionally characterized. The results showed that itaconate can block transamination activity of

BCAT and regulate catabolism of branched-chain amino acids in inflammatory macrophages.

Results

Profiling of ITA-interacting proteins by TPP

To profile ITA-interacting proteins by TPP (Fig. 1b), RAW 264.7 cells were suspended in PBS buffer and lysed by freezing–thawing with liquid nitrogen. After incubation with 1 mM itaconate or PBS buffer at room temperature, the resulting proteomes were split into 8 aliquots and subjected to a series of thermal stimulations at the indicated temperatures for 3 minutes. The soluble contents were extracted using centrifugation and analyzed using either gel-based or mass spectrometry (MS)-based methods. In the gel-based analysis, relative immunoblotting intensities were employed for quantification of individual proteins, while in the MS-based analysis, the samples were further digested by trypsin, labeled by using the IBTpro-16plex[42] labeling reagents and analyzed by LC-MS/MS to quantify protein abundance in each aliquot for a large number of proteins simultaneously. In both cases, thermal shift curves were fitted using the quantitative data and the T_m values with or without itaconate treatment were determined (Fig. 1b).

We performed the MS-based TPP experiments in three biological replicates. A total of 4912 proteins were quantified in at least one replicate and 3214 proteins were quantified across all three biological replicates. Based on these raw proteomic data, we obtained thermal shift curves for 2450 proteins under both conditions with high confidence after a strict filter was applied (Fig. 1c), and their T_m values demonstrated good correlation across the three biological replicates (Fig. S1†). To identify potential ITA-interacting targets, a volcano plot was created to display the ΔT_m value for each protein along with its statistical significance (Fig. 1c). Given that the global thermal stability of the RAW 264.7 proteome was not dramatically changed upon itaconate treatment as visualized by gel-based staining (Fig. S2†), we defined proteins with ΔT_m values exceeding 1 °C in all three biological replicates and a relatively significant P value ($|\Delta T_m \times (-\log_{10} P)| > 1.5$) as ITA-interacting targets. Finally, 190 proteins (8%) were found to meet these criteria and interestingly, all of them exhibited increasing thermal stability after ITA treatment (Fig. 1c and Table S1†).

As protein thermal stability can be affected by both covalent modification and non-covalent interactions of itaconate, we cross-checked with a list of 862 covalently itaconated proteins (with 1131 itaconated cysteine sites) obtained by the bio-orthogonal ITalk probe[18] to further distinguish the covalent and non-covalent targets in the TPP data (Fig. 1c and Table S1†). A total of 35 proteins were found in both ITalk and TPP data, including a prominent example of peroxiredoxin 1 (PRDX1) that is essential for cellular redox control. In particular, C173 of PRDX1 was previously identified to undergo itaconation, and mutation of this cysteine inhibited the formation of the PRX1 homodimer, which is associated with suppression of TNF-α-induced release.[43] The gel-based TPP showed that after itaconate treatment, the ΔT_m value of PRDX1 was changed by 2.0 ± 1.0 °C (Fig. 1d), which was consistent with the MS-based analysis (Fig. S3a†), further confirming the interaction between itaconate and PRDX1.

Aside from the covalent targets of itaconate, 155 proteins were identified specifically in the TPP profiling (Fig. 1c and Table S1†), which could be considered in principle as non-covalent binding targets of itaconate. Satisfyingly, this group included the known non-covalent target of itaconate, SDHA, which showed a ΔT_m of 1.8 ± 0.9 °C from the MS-based analysis and a ΔT_m of 2.0 ± 1.0 °C in the gel-based validation (Fig. 1e and S3b†). We also validated one novel target, lysine methyltransferase 2 (EFMT2), by overexpressing the protein, and the gel-based result demonstrated a similar change in thermal stability after itaconate treatment (Fig. 1f and S3c†).

Characterization of BCAT2 as a direct non-covalent target of ITA

We further performed the KEGG pathway enrichment analysis for these 155 TPP-specific ITA-interacting targets (Fig. 2a). The results showed that they were mainly involved in the citrate cycle, fatty acid metabolism and the pathway related to virus infection, all of which were associated with known functions of itaconate.[5] Additionally, there were two novel pathways discovered by TPP, including branched chain amino acids (BCAA) degradation and 2-oxocarboxylic acid metabolism, indicating that itaconate might play a regulatory role in these pathways. In particular, the mitochondrial branched-chain-amino-acid aminotransferase (BCAT2) drew our attention as the enzyme works in the initial phase of BCAA degradation and in the MS-based analysis, BCAT2 showed well-fitted melting curves with an ITA-induced ΔT_m of 1.5 ± 0.9 °C (Fig. 2b).

BCAT2 catalyzes the conversion from BCAAs, namely valine (VAL), leucine (LEU) and isoleucine (ILE), to their corresponding branched-chain-keto-acids (BCKAs), including 3-methyl-2-oxopentanoic acid (KMV), 3-methyl-2-oxobutanoic acid (KIV), and 4-methyl-2-oxopentanoic acid (KIC), and the reaction occurs with the concomitant conversion from α-ketoglutarate (AKG) to glutamate (GLU) (Fig. 2c).[44] The protein is known to regulate cancer proliferation[45,46] and chemokine release,[47] as well as cellular metabolism such as lipid metabolism.[48] Since the relevance of BCAT2 and itaconate has never been reported, we were therefore motivated to characterize their interaction and investigate the functional impact.

We first validated the thermal shifting result by the gel-based TPP assay in RAW 264.7 cell lysates. In both temperature- and concentration-based TPP experiments, itaconate could significantly increase thermal stability of BCAT2 (Fig. 2d and e). We further purified mouse BCAT2 (mBCAT2) and human BCAT2 (hBCAT2), and found that itaconate could also enhance thermal stability of these purified proteins (Fig. 2f and g), suggesting that this interaction between itaconate and BCAT2 is direct and conserved in mammalian cells.

To elucidate how itaconate specifically binds to BCAT2, we attempted to crystallize mBCAT2 or hBCAT2 in the presence of itaconate and successfully determined the structure of hBCAT2 in a complex with itaconate at 2.0 Å (Fig. 2h and Table S2†) (Protein Data Bank (PDB): 9LEP). The co-crystal structure of

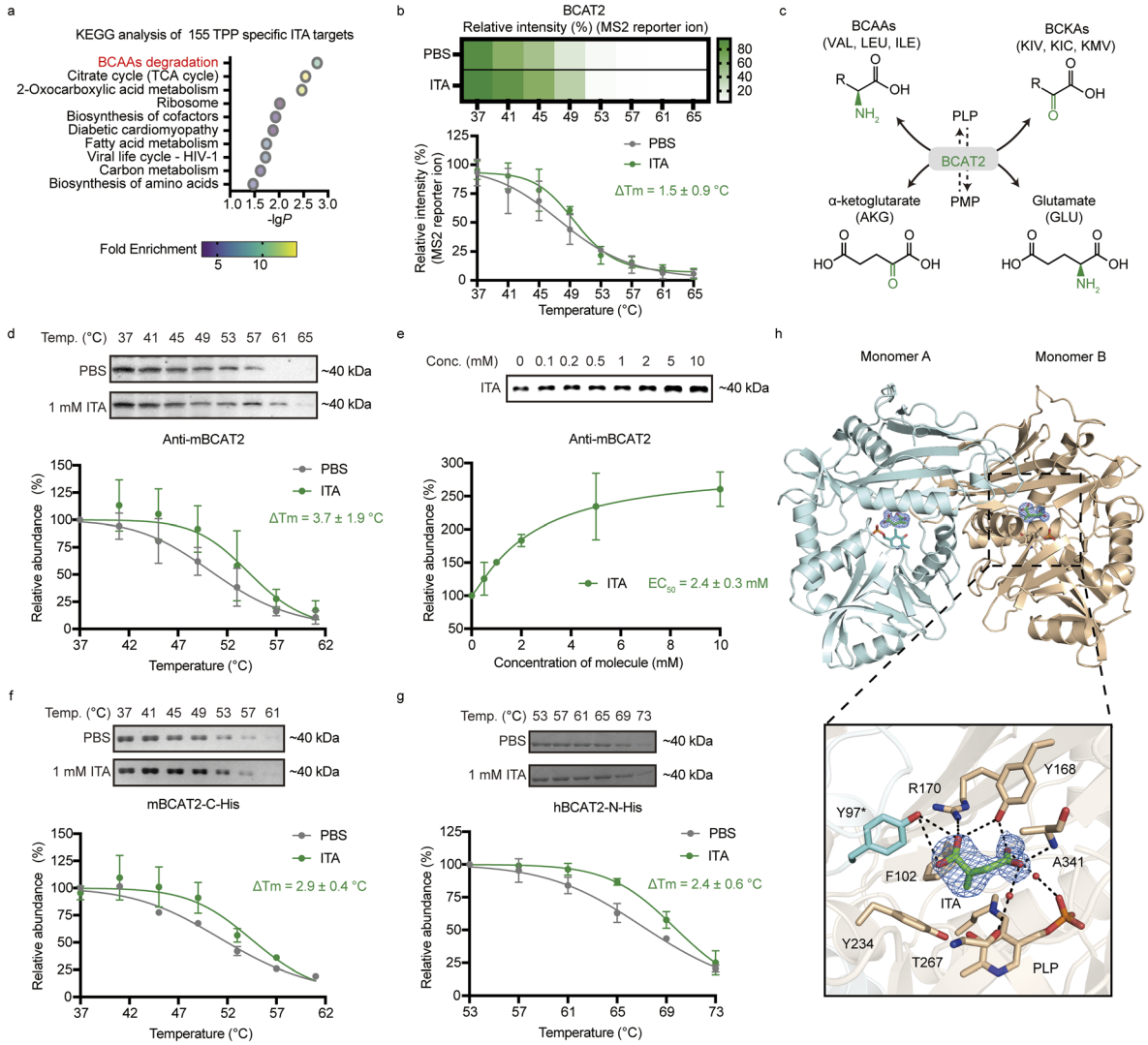

Fig. 2 Identification of BCAT2 as a direct and non-covalent binding target of ITA. (a) KEGG pathway analysis of the non-covalent ITA targets identified by TPP. (b) Thermal melting curve of BCAT2, as quantified by using MS2 reporter ion intensities from the TPP data. (c) Scheme showing the reaction catalyzed by BCAT2 in which BCAAs (VAL, LEU and ILE) are converted to BCKAs (KIV, KIC, and KMV) while AKG is converted to GLU. (d and e) In-gel verification of the interaction between BCAT2 and ITA in RAW 264.7 lysates using temperature-based (d) and concentration-based (e) TPP. (f and g) Gel-based temperature-related TPP for verifying the direct interaction between ITA and mBCAT2 (f) or hBCAT2 (g) using purified proteins. (h) hBCAT2 forms a dimer and ITA occupies the substrate binding pocket of hBCAT2. Top, the overall crystal structure of the hBCAT2 dimer complex. hBCAT2 is shown as ribbons and colored in pale cyan (monomer A) and wheat (monomer B). ITA and PLP are shown as sticks. Bottom, detailed interactions between hBCAT2 and ITA. A composite omit map is contoured at 1.0σ and shown as a marine mesh, revealing the presence of ITA. Hydrogen bonds are shown as black dashed lines. In (d–g), immunoblotting and quantification curves are shown at the top and bottom, respectively. Error bars stand for mean ± std, $n = 3$.

hBCAT2–ITA clearly showed that hBCAT2 forms a dimer and in each monomer, one molecule of itaconate was observed to directly bind to the pocket which was normally occupied by its native substrate, α-ketoglutarate. Specifically, itaconate formed several strong hydrogen bonds with hBCAT2 residues, including the sidechain phenol hydroxyl groups of Tyr168 from one monomer and Tyr97 from the other monomer, the side-chain guanidino group of Arg170, as well as the backbone amino group of Ala341. In addition, Phe102, Tyr234 and the cofactor pyridoxal phosphate (PLP) were involved in hydrophobic/van der Waals interactions with itaconate. Two water molecules were observed in the pocket, which also mediated a network of hydrogen bonds between itaconate and hBCAT2 residues. Together, all these data unambiguously supported that itaconate can non-covalently bind to hBCAT2.

Inhibition of the transaminase activity of BCAT2 by ITA

Given that itaconate and α-ketoglutarate shares the same binding pocket in BCAT2, we next investigated how the non-covalent binding of itaconate could regulate BCAT2's activity. Theoretically, BCAT2 is able to catalyze both the forward reaction and reverse reaction of the BCAAs–BCKAs conversion. To evaluate the activity of BCAT2, we used VAL and AKG as the

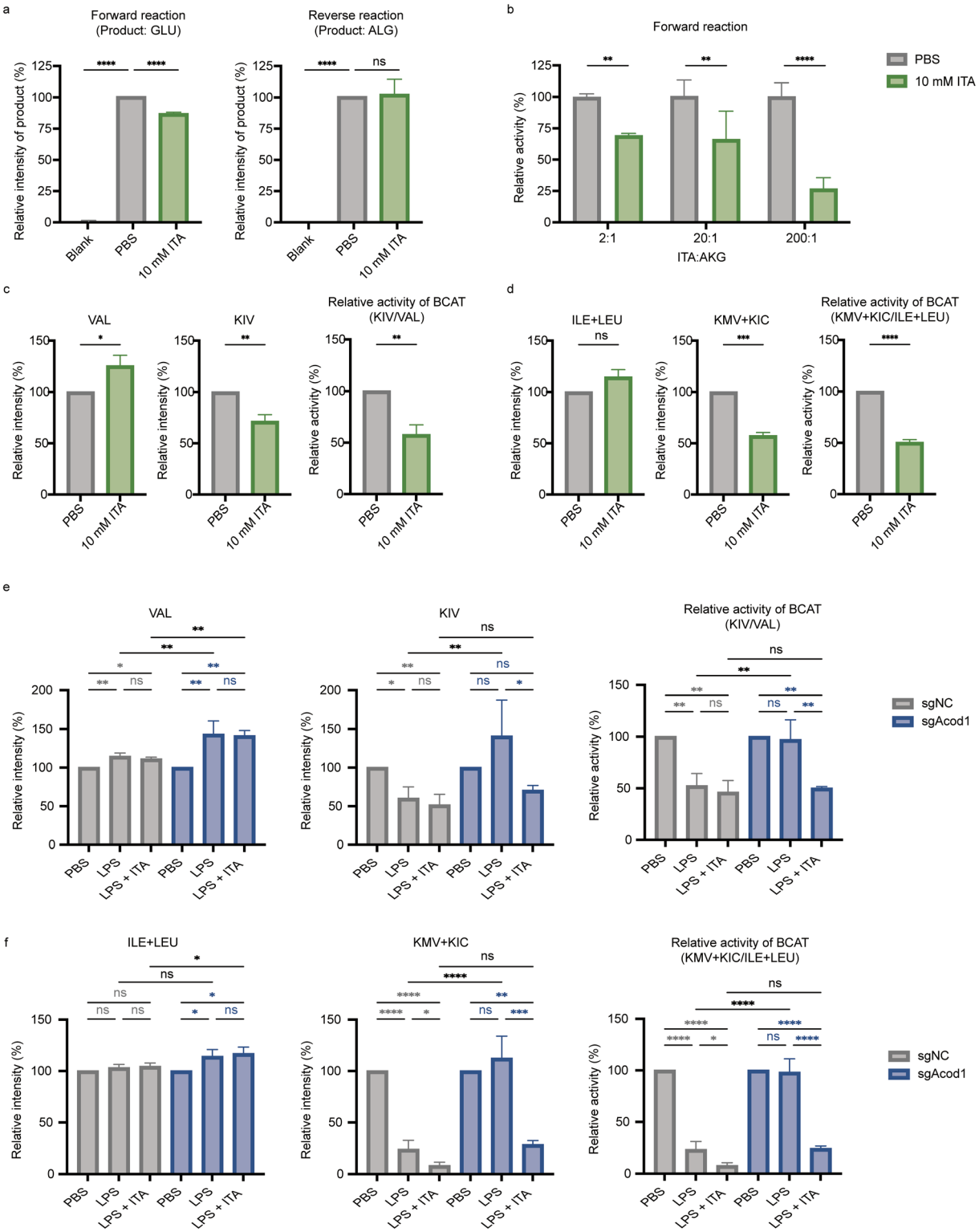

Fig. 3 ITA inhibits transaminase activity of BCAT2 and regulates BCAA catabolism. (a) ITA inhibited only the forward transamination reaction catalyzed by BCAT2. VAL and AKG were used as the substrates for the forward reaction, while KIV and GLU were used for the reverse reaction. GLU and AKG intensity was determined using LC-MS to reflect the activity of the two reactions. (b) Higher ITA/AKG ratios resulted in stronger inhibition of BCAT2 by ITA. (c and d) Exogenous ITA inhibited the transaminase activity of BCAT in living RAW 264.7 cells as measured by the levels of BCAAs and BCKAs as well as their ratios. (c) Conversion from VAL to KIV. (d) Conversion from LEU + ILE to KIC + KMV. (e and f) Endogenous ITA inhibited the transaminase activity of BCAT in living RAW 264.7 cells upon LPS stimulation. Levels of BCAAs and BCKAs were quantified by LC-MS and their ratios were calculated to reflect the transaminase activity of BCAT. The inhibitory effects were eliminated in the Acod1 knockout cell lines and could be rescued again by adding exogenous ITA. (e) Conversion from VAL to KIV. (f) Conversion from LEU + ILE to KIC + KMV. In (a–f), the results are from three independent experiments. *p < 0.05, **P < 0.01, ***P < 0.001, and ****P < 0.0001. Statistical differences were determined by ordinary one-way ANOVA.

substrates for measuring the forward reaction, and KIV and GLU as the substrates for measuring the reverse reaction. 10 mM itaconate was incubated with the purified mBCAT2 and corresponding substrates at 37 °C for 1 hour. The relative activity of mBCAT2 was determined by quantifying the amount of glutamate or α-ketoglutarate generated by the forward or reverse reaction using LC-MS. The results showed that itaconate could inhibit the forward activity of BCAT2 but did not affect that of the reverse reaction (Fig. 3a). With regard to the forward reaction, we also observed that a higher ITA/AKG ratio could result in more obvious inhibition (Fig. 3b), which indicated a model where itaconate could compete with α-ketoglutarate to inhibit activity of BCAT2. Detailed Michaelis–Menten kinetics analysis *in vitro* revealed a K_i value of 15.32 mM and a competitive inhibition mechanism (Fig. S4†). Considering that the local concentration of ITA might be higher in mitochondria, it is possible that BCAT2 will be inhibited in macrophages upon activation.

Interestingly, itaconate hardly changed the transamination activity of BCAT1 (Fig. S5a†), which is a cytosolic isoform of BCAT2, highlighting the unique isoform selectivity of itaconate against these two functionally similar enzymes. Consistent with this observation, purified BCAT1 did not show a thermal shift upon ITA incubation either (Fig. S5b†). To clarify this selectivity, the published structure of hBCAT1 (PDB: 7NWA) and our hBCAT2 were aligned for comparison. We noticed a different loop region outside the binding pocket (Pro192-Tyr193 in hBCAT1 and Ala199-Tyr200 in hBCAT2) (Fig. S6†) that may cause the selectivity of itaconate; however, a detailed structural study is necessary to fully explain this isoform selectivity.

We then investigated if the inhibition of BCAT2 by itaconate could also occur in living cells. RAW 264.7 cells were treated with 10 mM itaconate for 12 hours as in a previous study,[49] and the cellular metabolome was extracted using 80% methanol. The relative abundance of BCAAs, BCKAs, glutamate and α-ketoglutarate was quantified by LC-MS and the ratios of the corresponding BCKAs/BCAAs were calculated to reflect the transamination activity of BCAT. As expected, we observed a decreased level of BCKAs and an increased level of BCAAs after itaconate treatment, suggesting that itaconate could indeed inhibit BCAT's activity and interfere with BCAA metabolism in living cells (Fig. 3c and d). Surprisingly, we noticed that the level of AKG was also decreased after itaconate treatment (Fig. S7†). This change might be caused by other influenced proteins in the AKG metabolism such as IDH3a, which is an AKG synthase and was identified as an ITA target in our TPP data.

As itaconate is significantly up-regulated during pathogen inflection and inflammation, we next examined the alteration of BCAT activity and BCAA metabolism in lipopolysaccharide (LPS) activated macrophages. When macrophage cells were treated with 100 ng per mL LPS for 12 hours, the expression of Acod1 was promoted, resulting in the elevated production of endogenous itaconate as expected. To confirm that the inhibitory effect was solely dependent on itaconate, we also knocked out Acod1 in macrophages ("sgACOD1") by using CRISPR-Cas9,[21] which effectively eliminated the cellular production of itaconate under LPS induction in comparison with the control cells ("sgNC") (Fig. S8†). Along with the accumulation of itaconate, the forward activity of BCAT in the sgNC cells dropped, resulting in the reduction of KIV and accumulation of VAL (Fig. 3e and f). Satisfyingly, the change in BCAAs and BCKAs as well as the inhibited activity of BCAT was no longer observed in the sgACOD1 cells upon stimulation by LPS and the trend was reversed by adding exogenous itaconate to inhibit the activity of BCAT again (Fig. 3e and f). Collectively, these results indicated that itaconate generated by Acod1 was the key metabolite for regulating BCAT's activity and BCAA metabolism in LPS-activated inflammatory macrophages.

Conclusions

As one of the key immunoregulatory metabolites in macrophages, itaconate can bind to pivotal proteins to regulate their functions and associated biological processes. Here, we successfully identified itaconate-interacting proteins in macrophages by thermal proteome profiling, which provided more hints for deciphering the versatile functions of itaconate.

As chemical derivation would alter the natural reactivity of itaconate[7,49] and might prevent the formation of hydrogen bonds with amino acids in specific binding pockets of targets,[14,24] it is crucial to identify its targets using the unmodified molecules. While we have identified both non-covalent and covalent targets of itaconate with using TPP in this study, other advanced proteomic strategies such as LIP-MS,[50] TRAP,[51] ipHSA[52] and PELSA[34] would also be valuable for the identification and cross-validation of more itaconate targets, which will help overcome the problem of both false-positive and false-negative targets by the inherent limitation of TPP. In addition, while we attempted to distinguish non-covalent targets by comparing with the ITalk-captured itaconation targets[18] for simplicity, highly specific antibodies or probes are still highly desired to directly capture endogenous itaconation proteins at the proteome level. Given that itaconate binds to the BCAT2's pocket and is unlikely to be converted due to the lack of the α-keto acid moiety, it might be interesting to perform comparative profiling of itaconate with similar dicarboxylate metabolites to characterize their overlapping and unique interactome landscapes in living cells.

Subsequent functional research is also needed to focus on investigating in depth the biological impact of the BCAT2–ITA interaction. Non-covalent binding mode is often associated with reversible inhibition, which means that the inhibition on BCAT might vary depending on the level of itaconate during the inflammation or infection process. Additionally, recent studies also showed that BCAAs and BCAKs have different immune regulatory roles.[44,53,54] Therefore, a systematic investigation might be required to better understand the relation between BCAT2–ITA interaction and inflammation. Furthermore, BCAA metabolism is also reported to be linked to fatty acid metabolism and β-oxidation.[48] These two crucial biological processes have been shown to be regulated by itaconate, which results in a weight-reducing effect in the obese mouse model.[17] Hence, it is reasonable to speculate that there is a link between this BCAT2–ITA interaction and the weight-reducing effect. We

envisage that the chemoproteomic study presented here will offer valuable resources and novel clues to study itaconate-interacting proteins to better understand the versatile functions of this intriguing immunoregulatory metabolite.

Data availability

The MS proteomics data were deposited at the ProteomeXchange Consortium (**http://proteomecentral.proteomexchange.org**) *via* the iProX partner repository with the dataset identifier PXD060673. Source data are provided with this paper.

Author contributions

Y. M. and C. W. conceived the project. Y. M. conducted most of the chemoproteomic and biochemical experiments. J. X. guided and supervised T. W and C. Z. to solve the structure of hBCAT2–ITA. A. Y. helped purify mBCAT2 and hBCAT2 mutants. Y. L. developed computational algorithms to analyze the iBT proteomic data. Y. M. and C. W. analyzed the data and wrote the manuscript with input from all authors.

Conflicts of interest

There are no conflicts to declare.

Acknowledgements

We thank the Computing Platform of the Center for Life Science for supporting the proteomics data analysis. We thank the National Center for Protein Sciences at Peking University for assistance with protein crystallization and the staff of the Shanghai Synchrotron Radiation Facility for assistance with X-ray data collection. C. W. acknowledges the support from the National Natural Science Foundation of China (22525071, 22361142837, and 22321005), the Ministry of Science and Technology (2022YFA1304700), the Beijing National Laboratory for Molecular Sciences (BNLMS-CXTD-202401) and the PKUSZ-AI4S program.

References

1 K. Willmann and L. F. Moita, Physiologic disruption and metabolic reprogramming in infection and sepsis, *Cell Metab.*, 2024, **36**, 927–946.
2 G. Rosenberg, S. Riquelme, A. Prince and R. Avraham, Immunometabolic crosstalk during bacterial infection, *Nat. Microbiol.*, 2022, **7**, 497–507.
3 A. Michelucci, T. Cordes, J. Ghelfi, A. Pailot, N. Reiling, O. Goldmann, T. Binz, A. Wegner, A. Tallam, A. Rausell, M. Buttini, C. L. Linster, E. Medina, R. Balling and K. Hiller, Immune-responsive gene 1 protein links metabolism to immunity by catalyzing itaconic acid production, *Proc. Natl. Acad. Sci. U. S. A.*, 2013, **110**, 7820–7825.
4 C. L. Strelko, W. Lu, F. J. Dufort, T. N. Seyfried, T. C. Chiles, J. D. Rabinowitz and M. F. Roberts, Itaconic Acid Is a Mammalian Metabolite Induced during Macrophage Activation, *J. Am. Chem. Soc.*, 2011, **133**, 16386–16389.
5 D. Ye, P. Wang, L.-L. Chen, K.-L. Guan and Y. Xiong, Itaconate in host inflammation and defense, *Trends Endocrinol. Metab.*, 2024, **35**, 586–606.
6 E. A. Day and L. A. J. O'Neill, Protein targeting by the itaconate family in immunity and inflammation, *Biochem. J.*, 2022, **479**, 2499–2510.
7 A. F. McGettrick and L. A. J. O'Neill, Two for the price of one: itaconate and its derivatives as an anti-infective and anti-inflammatory immunometabolite, *Curr. Opin. Immunol.*, 2023, **80**, 102268.
8 S. A. Riquelme, K. Liimatta, T. Wong Fok Lung, B. Fields, D. Ahn, D. Chen, C. Lozano, Y. Sáenz, A.-C. Uhlemann, B. C. Kahl, C. J. Britto, E. DiMango and A. Prince, Pseudomonas aeruginosa Utilizes Host-Derived Itaconate to Redirect Its Metabolism to Promote Biofilm Formation, *Cell Metab.*, 2020, **31**, 1091–1106.
9 V. Lampropoulou, A. Sergushichev, M. Bambouskova, S. Nair, E. E. Vincent, E. Loginicheva, L. Cervantes-Barragan, X. Ma, S. C. Huang, T. Griss, C. J. Weinheimer, S. Khader, G. J. Randolph, E. J. Pearce, R. G. Jones, A. Diwan, M. S. Diamond and M. N. Artyomov, Itaconate Links Inhibition of Succinate Dehydrogenase with Macrophage Metabolic Remodeling and Regulation of Inflammation, *Cell Metab.*, 2016, **24**, 158–166.
10 S. T. Liao, C. Han, D. Q. Xu, X. W. Fu, J. S. Wang and L. Y. Kong, 4-Octyl itaconate inhibits aerobic glycolysis by targeting GAPDH to exert anti-inflammatory effects, *Nat. Commun.*, 2019, **10**, 5091.
11 M. Bambouskova, L. Gorvel, V. Lampropoulou, A. Sergushichev, E. Loginicheva, K. Johnson, D. Korenfeld, M. E. Mathyer, H. Kim, L.-H. Huang, D. Duncan, H. Bregman, A. Keskin, A. Santeford, R. S. Apte, R. Sehgal, B. Johnson, G. K. Amarasinghe, M. P. Soares, T. Satoh, S. Akira, T. Hai, C. de Guzman Strong, K. Auclair, T. P. Roddy, S. A. Biller, M. Jovanovic, E. Klechevsky, K. M. Stewart, G. J. Randolph and M. N. Artyomov, Electrophilic properties of itaconate and derivatives regulate the IκBζ–ATF3 inflammatory axis, *Nature*, 2018, **556**, 501–504.
12 M. C. Runtsch, S. Angiari, A. Hooftman, R. Wadhwa, Y. Zhang, Y. Zheng, J. S. Spina, M. C. Ruzek, M. A. Argiriadi, A. F. McGettrick, R. S. Mendez, A. Zotta, C. G. Peace, A. Walsh, R. Chirillo, E. Hams, P. G. Fallon, R. Jayaraman, K. Dua, A. C. Brown, R. Y. Kim, J. C. Horvat, P. M. Hansbro, C. Wang and L. A. J. O'Neill, Itaconate and itaconate derivatives target JAK1 to suppress alternative activation of macrophages, *Cell Metab.*, 2022, **34**, 487–501.
13 E. L. Mills, D. G. Ryan, H. A. Prag, D. Dikovskaya, D. Menon, Z. Zaslona, M. P. Jedrychowski, A. S. H. Costa, M. Higgins, E. Hams, J. Szpyt, M. C. Runtsch, M. S. King, J. F. McGouran, R. Fischer, B. M. Kessler, A. F. McGettrick, M. M. Hughes, R. G. Carroll, L. M. Booty, E. V. Knatko, P. J. Meakin, M. L. J. Ashford, L. K. Modis, G. Brunori,

D. C. Sévin, P. G. Fallon, S. T. Caldwell, E. R. S. Kunji, E. T. Chouchani, C. Frezza, A. T. Dinkova-Kostova, R. C. Hartley, M. P. Murphy and L. A. O'Neill, Itaconate is an anti-inflammatory metabolite that activates Nrf2 via alkylation of KEAP1, *Nature*, 2018, **556**, 113–117.

14 L. L. Chen, C. Morcelle, Z. L. Cheng, X. Chen, Y. Xu, Y. Gao, J. Song, Z. Li, M. D. Smith, M. Shi, Y. Zhu, N. Zhou, M. Cheng, C. He, K. Y. Liu, G. Lu, L. Zhang, C. Zhang, J. Zhang, Y. Sun, T. Qi, Y. Lyu, Z. Z. Ren, X. M. Tan, J. Yin, F. Lan, Y. Liu, H. Yang, M. Qian, C. Duan, X. Chang, Y. Zhou, L. Shen, A. S. Baldwin, K. L. Guan, Y. Xiong and D. Ye, Itaconate inhibits TET DNA dioxygenases to dampen inflammatory responses, *Nat. Cell Biol.*, 2022, **24**, 353–363.

15 R. A. Frieler, T. M. Vigil, J. Song, C. Leung, D. R. Goldstein, C. N. Lumeng and R. M. Mortensen, Aconitate decarboxylase 1 regulates glucose homeostasis and obesity in mice, *Obesity*, 2022, **30**, 1818–1830.

16 X. Zhang, Y. Zhi, X. Zan, K. Fan, K. Chen, S. Zhao, X. Dai, L. Li, Y. Yang, K. Hu, X. Gong and L. Zhang, Immune response gene 1 deficiency aggravates high fat diet-induced nonalcoholic fatty liver disease via promotion of redox-sensitive AKT suppression, *Biochim. Biophys. Acta, Mol. Basis Dis.*, 2023, **1869**, 166656.

17 Z. Yu, X. Li, Y. Quan, J. Chen, J. Liu, N. Zheng, S. Liu, Y. Wang, W. Liu, C. Qiu, Y. Wang, R. Zheng and J. Qin, Itaconate alleviates diet-induced obesity via activation of brown adipocyte thermogenesis, *Cell Rep.*, 2024, **43**, 114142.

18 W. Qin, Y. Zhang, H. Tang, D. Liu, Y. Chen, Y. Liu and C. Wang, Chemoproteomic Profiling of Itaconation by Bioorthogonal Probes in Inflammatory Macrophages, *J. Am. Chem. Soc.*, 2020, **142**, 10894–10898.

19 W. Qin, K. Qin, Y. Zhang, W. Jia, Y. Chen, B. Cheng, L. Peng, N. Chen, Y. Liu, W. Zhou, Y.-L. Wang, X. Chen and C. Wang, S-glycosylation-based cysteine profiling reveals regulation of glycolysis by itaconate, *Nat. Chem. Biol.*, 2019, **15**, 983–991.

20 Y. Zhang, W. Qin, D. Liu, Y. Liu and C. Wang, Chemoproteomic profiling of itaconations in Salmonella, *Chem. Sci.*, 2021, **12**, 6059–6063.

21 Z. Liu, D. Liu and C. Wang, *In situ* chemoproteomic profiling reveals itaconate inhibits *de novo* purine biosynthesis in pathogens, *Cell Rep.*, 2024, **43**, 114737.

22 C. Wei, Z. Xiao, Y. Zhang, Z. Luo, D. Liu, L. Hu, D. Shen, M. Liu, L. Shi, X. Wang, T. Lan, Q. Dai, J. Liu, W. Chen, Y. Zhang, Q. Sun, W. Wu, P. Wang, C. Zhang, J. Hu, C. Wang, F. Yang and Q. Li, Itaconate protects ferroptotic neurons by alkylating GPx4 post stroke, *Cell Death Differ.*, 2024, **31**, 983–998.

23 D. Liu, W. Xiao, H. Li, Y. Zhang, S. Yuan, C. Li, S. Dong and C. Wang, Discovery of Itaconate-Mediated Lysine Acylation, *J. Am. Chem. Soc.*, 2023, **145**, 12673–12681.

24 F. Chen, W. A. M. Elgaher, M. Winterhoff, K. Büssow, F. H. Waqas, E. Graner, Y. Pires-Afonso, L. Casares Perez, L. de la Vega, N. Sahini, L. Czichon, W. Zobl, T. Zillinger, M. Shehata, S. Pleschka, H. Bähre, C. Falk, A. Michelucci, S. Schuchardt, W. Blankenfeldt, A. K. H. Hirsch and F. Pessler, Citraconate inhibits ACOD1 (IRG1) catalysis, reduces interferon responses and oxidative stress, and modulates inflammation and cell metabolism, *Nat. Metab.*, 2022, **4**, 534–546.

25 M. M. Savitski, F. B. Reinhard, H. Franken, T. Werner, M. F. Savitski, D. Eberhard, D. Martinez Molina, R. Jafari, R. B. Dovega, S. Klaeger, B. Kuster, P. Nordlund, M. Bantscheff and G. Drewes, Tracking cancer drugs in living cells by thermal profiling of the proteome, *Science*, 2014, **346**, 1255784.

26 H. Franken, T. Mathieson, D. Childs, G. M. A. Sweetman, T. Werner, I. Tögel, C. Doce, S. Gade, M. Bantscheff, G. Drewes, F. B. M. Reinhard, W. Huber and M. M. Savitski, Thermal proteome profiling for unbiased identification of direct and indirect drug targets using multiplexed quantitative mass spectrometry, *Nat. Protoc.*, 2015, **10**, 1567–1593.

27 K. V. M. Huber, K. M. Olek, A. C. Müller, C. S. H. Tan, K. L. Bennett, J. Colinge and G. Superti-Furga, Proteome-wide drug and metabolite interaction mapping by thermal-stability profiling, *Nat. Methods*, 2015, **12**, 1055–1057.

28 I. Becher, T. Werner, C. Doce, E. A. Zaal, I. Tögel, C. A. Khan, A. Rueger, M. Muelbaier, E. Salzer, C. R. Berkers, P. F. Fitzpatrick, M. Bantscheff and M. M. Savitski, Thermal profiling reveals phenylalanine hydroxylase as an off-target of panobinostat, *Nat. Chem. Biol.*, 2016, **12**, 908–910.

29 Y. Tu, L. Tan, H. Tao, Y. Li and H. Liu, CETSA and thermal proteome profiling strategies for target identification and drug discovery of natural products, *Phytomedicine*, 2023, **116**, 154862.

30 F. B. M. Reinhard, D. Eberhard, T. Werner, H. Franken, D. Childs, C. Doce, M. F. Savitski, W. Huber, M. Bantscheff, M. M. Savitski and G. Drewes, Thermal proteome profiling monitors ligand interactions with cellular membrane proteins, *Nat. Methods*, 2015, **12**, 1129–1131.

31 M. Kalxdorf, I. Günthner, I. Becher, N. Kurzawa, S. Knecht, M. M. Savitski, H. C. Eberl and M. Bantscheff, Cell surface thermal proteome profiling tracks perturbations and drug targets on the plasma membrane, *Nat. Methods*, 2021, **18**, 84–91.

32 S. Sridharan, N. Kurzawa, T. Werner, I. Günthner, D. Helm, W. Huber, M. Bantscheff and M. M. Savitski, Proteome-wide solubility and thermal stability profiling reveals distinct regulatory roles for ATP, *Nat. Commun.*, 2019, **10**, 1155.

33 Y. T. Lim, N. Prabhu, L. Dai, K. D. Go, D. Chen, L. Sreekumar, L. Egeblad, S. Eriksson, L. Chen, S. Veerappan, H. L. Teo, C. S. H. Tan, J. Lengqvist, A. Larsson, R. M. Sobota and P. Nordlund, An efficient proteome-wide strategy for discovery and characterization of cellular nucleotide-protein interactions, *PLoS One*, 2018, **13**, e0208273.

34 K. Li, S. Chen, K. Wang, Y. Wang, L. Xue, Y. Ye, Z. Fang, J. Lyu, H. Zhu, Y. Li, T. Yu, F. Yang, X. Zhang, S. Guo, C. Ruan, J. Zhou, Q. Wang, M. Dong, C. Luo and M. Ye, A peptide-centric local stability assay enables proteome-scale identification of the protein targets and binding regions of diverse ligands, *Nat. Methods*, 2025, **22**, 278–282.

35 K. J. Li, Y. Y. Ye, X. L. Zhang, J. H. Zhou, Y. N. Li and M. L. Ye, Identification of the binding proteins of organic acid metabolites by matrix thermal shift assay, *Sepu*, 2024, **42**, 702–710.

36 X. Zeng, T. Wei, X. Wang, Y. Liu, Z. Tan, Y. Zhang, T. Feng, Y. Cheng, F. Wang, B. Ma, W. Qin, C. Gao, J. Xiao and C. Wang, Discovery of metal-binding proteins by thermal proteome profiling, *Nat. Chem. Biol.*, 2024, **20**, 770–778.

37 J. X. Huang, G. Lee, K. E. Cavanaugh, J. W. Chang, M. L. Gardel and R. E. Moellering, High throughput discovery of functional protein modifications by Hotspot Thermal Profiling, *Nat. Methods*, 2019, **16**, 894–901.

38 C. M. Potel, N. Kurzawa, I. Becher, A. Typas, A. Mateus and M. M. Savitski, Impact of phosphorylation on thermal stability of proteins, *Nat. Methods*, 2021, **18**, 757–759.

39 I. R. Smith, K. N. Hess, A. A. Bakhtina, A. S. Valente, R. A. Rodríguez-Mias and J. Villén, Identification of phosphosites that alter protein thermal stability, *Nat. Methods*, 2021, **18**, 760–762.

40 D. T. King, J. E. Serrano-Negrón, Y. Zhu, C. L. Moore, M. D. Shoulders, L. J. Foster and D. J. Vocadlo, Thermal Proteome Profiling Reveals the O-GlcNAc-Dependent Meltome, *J. Am. Chem. Soc.*, 2022, **144**, 3833–3842.

41 C. Sayago, J. Sánchez-Wandelmer, F. García, B. Hurtado, V. Lafarga, P. Prieto, E. Zarzuela, P. Ximénez-Embún, S. Ortega, D. Megías, O. Fernández-Capetillo, M. Malumbres and J. Munoz, Decoding protein methylation function with thermal stability analysis, *Nat. Commun.*, 2023, **14**, 3016.

42 Y. Ren, Y. He, Z. Lin, J. Zi, H. Yang, S. Zhang, X. Lou, Q. Wang, S. Li and S. Liu, Reagents for Isobaric Labeling Peptides in Quantitative Proteomics, *Anal. Chem.*, 2018, **90**, 12366–12371.

43 L. Mullen, E. M. Hanschmann, C. H. Lillig, L. A. Herzenberg and P. Ghezzi, Cysteine Oxidation Targets Peroxiredoxins 1 and 2 for Exosomal Release through a Novel Mechanism of Redox-Dependent Secretion, *Mol. Med.*, 2015, **21**, 98–108.

44 A. Dimou, V. Tsimihodimos and E. Bairaktari, The Critical Role of the Branched Chain Amino Acids (BCAAs) Catabolism-Regulating Enzymes, Branched-Chain Aminotransferase (BCAT) and Branched-Chain α-Keto Acid Dehydrogenase (BCKD), in Human Pathophysiology, *Int. J. Mol. Sci.*, 2022, **23**, 4022.

45 J. Li, M. Yin, D. Wang, J. Wang, M.-Z. Lei, Y. Zhang, Y. Liu, L. Zhang, S.-W. Zou, L.-P. Hu, Z.-G. Zhang, Y.-P. Wang, W.-Y. Wen, H.-J. Lu, Z.-J. Chen, D. Su and Q.-Y. Lei, BCAT2-mediated BCAA catabolism is critical for development of pancreatic ductal adenocarcinoma, *Nat. Cell Biol.*, 2020, **22**, 167–174.

46 K. Wang, Z. Zhang, H.-I. Tsai, Y. Liu, J. Gao, M. Wang, L. Song, X. Cao, Z. Xu, H. Chen, A. Gong, D. Wang, F. Cheng and H. Zhu, Branched-chain amino acid aminotransferase 2 regulates ferroptotic cell death in cancer cells, *Cell Death Differ.*, 2021, **28**, 1222–1236.

47 Z. Cai, J. Chen, Z. Yu, H. Li, Z. Liu, D. Deng, J. Liu, C. Chen, C. Zhang, Z. Ou, M. Chen, J. Hu and X. Zu, BCAT2 Shapes a Noninflamed Tumor Microenvironment and Induces Resistance to Anti-PD-1/PD-L1 Immunotherapy by Negatively Regulating Proinflammatory Chemokines and Anticancer Immunity, *Adv. Sci.*, 2023, **10**, e2207155.

48 Q. X. Ma, W. Y. Zhu, X. C. Lu, D. Jiang, F. Xu, J. T. Li, L. Zhang, Y. L. Wu, Z. J. Chen, M. Yin, H. Y. Huang and Q. Y. Lei, BCAA–BCKA axis regulates WAT browning through acetylation of PRDM16, *Nat. Metab.*, 2022, **4**, 106–122.

49 A. Swain, M. Bambouskova, H. Kim, P. S. Andhey, D. Duncan, K. Auclair, V. Chubukov, D. M. Simons, T. P. Roddy, K. M. Stewart and M. N. Artyomov, Comparative evaluation of itaconate and its derivatives reveals divergent inflammasome and type I interferon regulation in macrophages, *Nat. Metab.*, 2020, **2**, 594–602.

50 I. Piazza, K. Kochanowski, V. Cappelletti, T. Fuhrer, E. Noor, U. Sauer and P. Picotti, A Map of Protein-Metabolite Interactions Reveals Principles of Chemical Communication, *Cell*, 2018, **172**, 358–372.

51 Y. Tian, N. Wan, H. Zhang, C. Shao, M. Ding, Q. Bao, H. Hu, H. Sun, C. Liu, K. Zhou, S. Chen, G. Wang, H. Ye and H. Hao, Chemoproteomic mapping of the glycolytic targetome in cancer cells, *Nat. Chem. Biol.*, 2023, **19**, 1480–1491.

52 X. Zhang, C. Ruan, Y. Wang, K. Wang, X. Liu, J. Lyu and M. Ye, Integrated Protein Solubility Shift Assays for Comprehensive Drug Target Identification on a Proteome-Wide Scale, *Anal. Chem.*, 2023, **95**, 13779–13787.

53 Y. Dong, X. Zhang, R. Miao, W. Cao, H. Wei, W. Jiang, R. Gao, Y. Yang, H. Sun and J. Qiu, Branched-chain amino acids promotes the repair of exercise-induced muscle damage via enhancing macrophage polarization, *Front Physiol*, 2022, **13**, 1037090.

54 L. S. Silva, G. Poschet, Y. Nonnenmacher, H. M. Becker, S. Sapcariu, A. C. Gaupel, M. Schlotter, Y. Wu, N. Kneisel, M. Seiffert, R. Hell, K. Hiller, P. Lichter and B. Radlwimmer, Branched-chain ketoacids secreted by glioblastoma cells via MCT1 modulate macrophage phenotype, *EMBO Rep.*, 2017, **18**, 2172–2185.